JGR Solid Earth

RESEARCH ARTICLE
10.1029/2018JB017274

Mantle-Derived Fluids in the East Java Sedimentary Basin, Indonesia

Alexandra Zaputlyaeva[1], Adriano Mazzini[1], Antonio Caracausi[2], and Alessandra Sciarra[3,4]

[1]Centre for Earth Evolution and Dynamics (CEED), University of Oslo, Oslo, Norway, [2]Istituto Nazionale di Geofisica e Vulcanologia (INGV), Palermo, Italy, [3]Istituto Nazionale di Geofisica e Vulcanologia (INGV), Rome, Italy, [4]Consiglio Nazionale delle Ricerche—Istituto di Geologia Ambientale e Geoingegneria, Rome, Italy

Key Points:
- Advective migration of mantle-derived volatiles occurs through faults and fractures in the sedimentary basin
- Mantle-derived volatiles are trapped within shallow hydrocarbon accumulations
- Biodegradation processes in the hydrocarbon reservoirs and gas dissolution in the formation water mask the abiogenic carrier gas

Correspondence to:
A. Zaputlyaeva,
alexandra.zaputlyaeva@geo.uio.no

Citation:
Zaputlyaeva, A., Mazzini, A., Caracausi, A., & Sciarra, A. (2019). Mantle-derived fluids in the East Java sedimentary basin, Indonesia. *Journal of Geophysical Research: Solid Earth*, *124*, 7962–7977. https://doi.org/10.1029/2018JB017274

Received 29 DEC 2018
Accepted 8 JUL 2019
Accepted article online 16 JUL 2019
Published online 14 AUG 2019

Abstract The Tertiary back-arc sedimentary basin in East Java (Indonesia) hosts a large variety of piercement structures and hydrocarbon fields. Some of the latter (Wunut, Tanggulangin, Carat, Watudakon) are located a few kilometers away from the Arjuno-Welirang volcanic complex and neighboring Lusi, the largest active sediment-hosted hydrothermal system on Earth. In order to investigate interactions between volcanic and sedimentary settings, we performed gas sampling on these four shallow (200- to 1,000-m depth) petroleum fields. The fields around Lusi are dominated by thermogenic gas that was altered during biodegradation processes. The helium isotope ratios ($^3He/^4He$) are as high as 6.7 R_A, which is remarkably similar to those measured at the fumaroles of the adjacent volcanic complex (R = 7.3 R_A) and at the Lusi site (up to 6.5 R_A). This highlights the pervasive outgassing of mantle-derived fluids in the sedimentary basin. Despite these two systems sharing the same mantle-derived helium source, their hydrocarbons have two different genetic histories: Lusi hydrocarbon gas has been more recently generated and is less molecularly and isotopically fractionated, while the gas trapped in the reservoirs is older and more altered. Unlike Lusi, the hydrocarbon fields contain small amounts of CO_2 resulting from biodegradation processes. The Watukosek fault system, originating from the Arjuno-Welirang volcanic complex and extending toward the northeast of Java, intersects Lusi and the hydrocarbon fields. This network of faults controls the migration of mantle-derived fluids within the sedimentary basin, feeding the focused venting at the Lusi site and promoting the slower and pervasive migration in the reservoirs.

Plain Language Summary The East Java sedimentary basin is located to the north of the E-W trending chain of active volcanoes that transects the Java Island. The basin hosts numerous oil and gas fields, as well as buried diapirs and active mud eruption sites. This study focuses on gas geochemical analyses from the surface seeps and four shallow petroleum fields located around Lusi, the largest active mud eruption on Earth. Comparative results show that the biodegraded thermogenic gas in the reservoirs differs from the thermogenic gas vented at Lusi and its surrounding seeps. In contrast, helium gas analysis from the hydrocarbon reservoirs, the Lusi eruption and satellite seeps, and from the fumaroles at the neighboring Arjuno-Welirang volcanic complex share a common mantle-derived component. Available seismic data from the region confirm that a system of faults (Watukosek fault system), extending from the volcanic complex toward the sedimentary basin, promotes the migration of mantle-derived fluids through a broad area in the East Java sedimentary basin. These results confirm that the Lusi system is fueled by the lateral migration of mantle-derived fluids that trigger reactions within the organic rich formations in the sedimentary basin.

1. Introduction

The presence of mantle-derived volatiles is typically associated with degassing of volcanic plumes, diffuse emissions around volcanic edifices, mid-ocean ridges, modern continental rifts, or deep active fault systems (e.g., Caracausi et al., 2015; Caracausi & Sulli, 2019; Halldórsson et al., 2013; Lee et al., 2016; Sano & Fischer, 2013). These systems are commonly dominated by water and CO_2 and contain trace amounts of noble gases with specific isotopic compositions that indicate a mantle-derived origin (Moreira & Kurz, 2013). Some sedimentary basins have been documented to host hydrocarbon (HC) reservoirs containing mantle-derived volatiles, for example, Green Tuff Basin in Japan, Okinawa Trough in East China Sea,

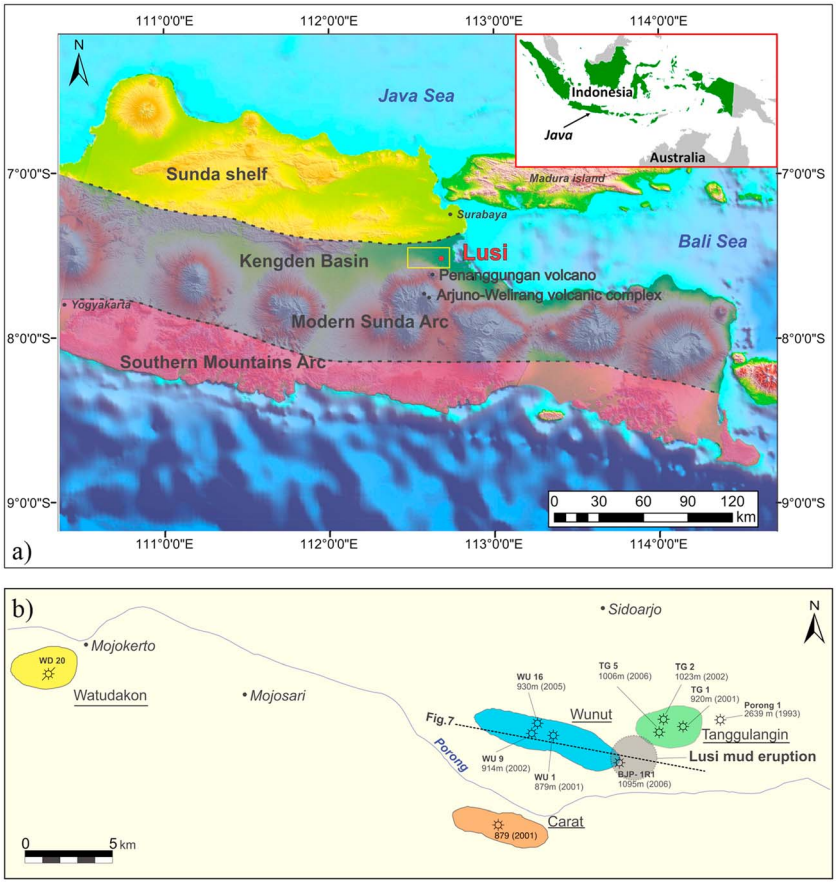

Figure 1. (a) Digital elevation model of the central and eastern Java with main tectonic zones (redrawn and modified after Istadi et al., 2009; Smyth et al., 2008); the yellow rectangle indicates the study area depicted at (b); inset map of Indonesia; (b) location of the sampled wells in the Wunut, Tanggulangin, Carat, Watudakon fields, bottom hole depth, and drilling year. Dashed line indicates the location of the seismic profile, shown at Figure 7.

Sacramento Basin and Escanaba Trough in California, and multiple basins distributed in New Zealand, Thailand, Indonesia, Philippines, Taiwan, and Kamchatka peninsula (Ishibashi et al., 2002; Jenden et al., 1993; Kamenskiy et al., 1971; Poreda et al., 1986; Sakata et al., 1997; Xu et al., 1995). Thermogenic gas produced at these localities ($\delta^{13}C_{CH4}$ between −30‰ and −60 ‰) was mainly generated by the thermal cracking of organic matter. Helium (hereafter He) isotope compositions at these reservoirs indicate the presence of mantle-derived volatiles (R = 0.2–7.7 R_A, where R = $^3He/^4He$ of the sample, R_A = $^3He/^4He$ of air (1.4×10^{-6})).

A setting similar to those described above is encountered in the Tertiary-aged East Java sedimentary basin, north of the volcanic Sunda Arc, formed by the subduction of the Indo-Australian plate beneath the Eurasian continental plate (Hall, 2002; Figure 1a). The basin is characterized by high sedimentation rates, deposition of organic-rich sediments, and volcaniclastic and carbonate traps, resulting in the formation of a HC province with numerous oil and gas fields and diffused surface and subsurface piercement structures (Istadi et al., 2012; Mazzini et al., 2018; Mazzini et al., 2007; Moscariello et al., 2018; Satyana & Purwaningsih, 2003a, 2003b). The basin bordered to the south by the Penanggungan, Arjuno-Welirang, and Bromo volcanoes and represents an ideal opportunity to investigate the relationship between mantle-derived volatiles and HC fluids in oil and gas reservoirs.

This region is also of particular interest because of the Lusi piercement, the world's largest active mud eruption neighboring the Holocene Penanggungan and Arjuno-Welirang volcanoes, situated, respectively, at 10 and 25 km to the southwest (Figures 1b and 2). Lusi (named after LUmpur, meaning mud in Indonesian, and SIdoarjo, the Local Regency) started its eruptive activity on the 29 May 2006 and has since been continuously

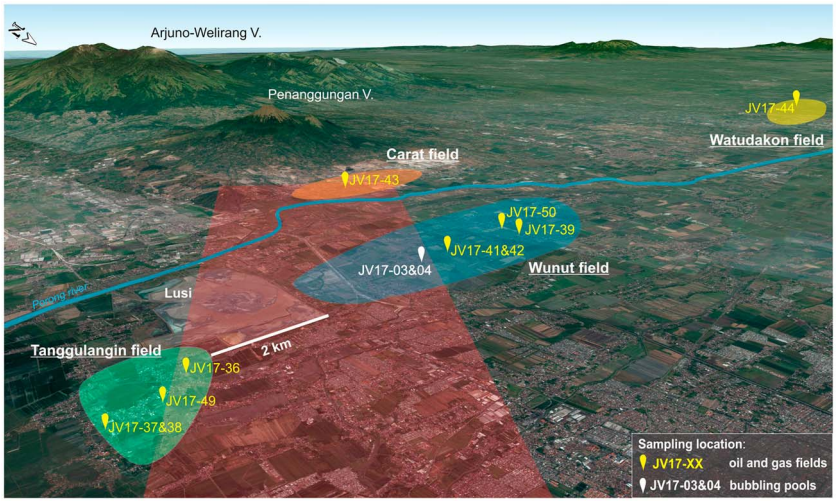

Figure 2. 3-D Google Earth view of the study area with indicated location of the oil and gas fields (color shaded areas), the sampling stations, and the Watukosek fault system (red shaded area).

bursting boiling water, gas, mud, oil, and rock clasts (Van Noorden, 2006). A set of targeted field campaigns has been completed since the beginning of the eruption to investigate the origin of the erupted fluids and the subsurface plumbing system (Miller & Mazzini, 2018, and references therein). Results revealed that outgassing boiling fluids at the Lusi surface contain evidence of hydrothermal waters and a mix of inorganic and organic gases, including geothermal (thermo-metamorphic and mantle-derived) and biotic (i.e., thermogenic methane) gases (Mazzini et al., 2012; Mazzini et al., 2018). Ambient noise tomography revealed a connection between the Arjuno-Welirang magma chamber and the Lusi conduit at around 4.5-km depth, indicating the migration of magmatic and hydrothermal fluids toward the sedimentary basin (Fallahi et al., 2017). These results confirmed that Lusi is indeed not a mud volcano but rather a sediment-hosted geothermal system (Mazzini & Etiope, 2017; Procesi et al., 2019). Sampling from the fumaroles of the Arjuno-Welirang volcanic complex provided further evidence of the connection between these two eruptive systems (Inguaggiato et al., 2018). The authors revealed that both the fumaroles of the Arjuno-Welirang and gas at the Lusi site contain magmatic volatiles with high ^{3}He abundance ($R = 7.3$ and 6.5 R_A, respectively). Furthermore, the Watukosek fault system (WFS), extending toward the northeast of the island from the Arjuno-Welirang volcanic complex (Figure 2), hosts Lusi and several mud volcanoes (Fallahi et al., 2017; Mazzini et al., 2009; Mazzini et al., 2012; Moscariello et al., 2018; Obermann et al., 2018; Sciarra et al., 2018). The authors indicate that this sinistral strike-slip system provides an ideal pathway for the propagation of the deep overpressured hydrothermal fluids toward the sedimentary basin and further to the surface.

This complex plumbing system and tectonic structures are largely controlling the past and present migration of fluids. Lusi is surrounded by three shallow oil and gas fields (Figures 1b and 2) that reflect the paleo-migration of HCs in the basin. Despite the obvious proximity between Lusi and these HC reservoirs, no dedicated studies have yet been conducted to investigate (1) if the HC gas currently erupted at Lusi is the same as that stored in the reservoirs, (2) if any correlation represents a potential connection between these two systems, and (3) whether the WFS could also provide a migration pathway for the mantle-derived fluids to the shallow reservoirs. This study aims to characterize the composition and origin of the gas trapped in the subsurface and to unravel the above questions by analyzing targeted samples.

2. Geological Setting

The East Java Basin is located on the southeastern margin of the Sunda plate, bounded to the south by the northward subduction of the Indian-Australian Plate. The subduction initiated in the Middle Eocene and resulted in the formation of two volcanic arcs: the Southern Mountain Arc (active between ca. 45 and

20 Ma) and Sunda Arc (active since ca. 12–10 Ma; Hall, 2013; Smyth et al., 2008). The axis of the Sunda Arc is located 50 km to the north from the older Southern Mountain Arc. The Arjuno-Welirang volcanic complex consists of Holocene stratovolcanoes, located in the eastern part of the Sunda Arc. Penanggungan is the northeasternmost volcano of this complex and is in the vicinity (~10 km) of the Lusi mud eruption and the studied oil and gas fields. The most recent recorded eruptive activity occurred at the Welirang volcano in 1952 (Global Volcanism Program, 2013). Currently, the crater is characterized by solfataric fields, with several hydrothermal seeps distributed on the flanks (Inguaggiato et al., 2018; Mazzini et al., 2012; Mazzini et al., 2018).

The East Java Basin comprises a complex of northeast to southwest trending troughs, developed during Late Eocene to Early Miocene due to the extensional regime of the Sunda plate (Doust & Noble, 2008). The sedimentary section contains more than 5 km of deposits, spanning in age from Eocene to recent, overlying the pre-Tertiary basement, with the maximum sediment thickness of 8–10 km in the Kengden graben (Hall et al., 2011; Kusumastuti et al., 1999; Martha et al., 2017). In the study area, the lithostratigraphic section is constrained by drilled boreholes, analyzed clasts erupted at the Lusi site, and by seismic surveys from the 1990s–2000s (Istadi et al., 2009; Malvoisin et al., 2018; Mazzini et al., 2018; Mazzini et al., 2007; Moscariello et al., 2018; Samankassou et al., 2018; Satyana & Purwaningsih, 2003b; Sharaf et al., 2005; Tingay, 2015). The sedimentary section constrained in the deepest well (BJP1, TVD 2,833 m) consists of (from top to down) the following:

1. recent alluvial sediments (intercalated sands, shales, and volcaniclastic sands and clays), 0–290 m;
2. volcaniclastic shales and sands of the Pucangan Formation, Pleistocene, 290–900 m;
3. bluish gray shales of the upper part of the Upper Kalibeng Formation, Pleistocene, 900–1,871 m; and
4. tight volcanic and volcaniclastic units of the lower part of the Upper Kalibeng Formation, Upper Pliocene-Pleistocene, 1,871 to at least ~2,833 m.

Lithostratigraphy below 2,833 m is based on regional studies, Lusi mud breccia analyses, and seismic data

1. marls and shales of the Tuban Formation, Lower-Upper Miocene, from >2,833 to ~3,250 m;
2. reefal and platform carbonates of the Kujung Formation, Upper Oligocene-Lower Miocene, from ~3,250 to ~3,800 m; and
3. organic-rich black shales of the Ngimbang Formation, Middle Eocene-Lower Oligocene, >3,800 m.

The basin is characterized by high sedimentation rates (0.7 km/Ma) since Late Pliocene, which resulted in fast burial and preservation of the semilithified deposits.

3. Petroleum System of the East Java Basin

The East Java Basin is a petroleum province with a total reserve volume of 1,830 Million Barrels of Oil Equivalent (Doust & Noble, 2008). The HC accumulations in the basin are confined to shallow volcaniclastic Pleistocene reservoirs (Pucangan Fm.), Miocene sands of the Ngrayong and Woncolo Formations, Upper Oligocene-Lower Miocene reefal carbonates of the Kujung Fm., and carbonates and sands of the Ngimbang Formation (Doust & Noble, 2008; Satyana & Purwaningsih, 2003b).

The main HC source rock is suggested to be the Middle Eocene-Lower Oligocene organic-rich shales, coals, and coaly shales of the Ngimbang Fm. (Devi et al., 2018; Satyana & Purwaningsih, 2003a). These sediments were deposited in a fluvio-deltaic to near-shore marine environment. Organic-rich shales of the Ngimbang Fm. contain up to 5.7 wt.% Total Organic Carbon (TOC) and coal bearing interval with TOC up to 67 wt.% (Satyana & Purwaningsih, 2003a).

The study area is located in the southern part of the East Java Basin, to the north of the Arjuno-Welirang volcanic complex and in the neighborhood of the Lusi eruption site. Three production HC fields, Wunut, Tanggulangin, and Carat, surrounding Lusi site were targeted for investigation. Here producing reservoir intervals are confined to the Pucangan Fm., 200- to 1,000-m depth, that was deposited as a northeastward prograding, volcaniclastic sedimentary wedge (Istadi et al., 2009; Kusumastuti et al., 1999). The Pucangan Fm. consists of predominantly fine-grained material (up to 80% of net shales) and layers of sandstones, 3–47 m thick (Kusumastuti et al., 1999). The intercalating shales seal the HC accumulations. The traps

are four-way dip closures with multiple reservoir layers. The lower intervals of the Pucangan Fm. contain oil, while the shallower units are gas prone. The measured thermal gradient in the wells varies from 2.8 to 4.9 °C/100 m.

4. Sampling and Analytical Procedures

During spring 2017, a gas sampling campaign was conducted in northeast Java with the aim to obtain surface and subsurface gas samples of the southern part of the East Java Basin. Two main settings and localities have been targeted (Figures 1b and 2). The first set of samples (Group 1) was collected from several production wells of targeted gas fields (Wunut, Tanggulangin, and Carat). Surface seeping gas was collected from bubbling pools, located above the Wunut field (Group 2). In addition, the Watudakon gas field (~36 km west of the Lusi on the outskirts of the Arjuno-Welirang volcanic complex) was sampled (Group 3). Formation waters from the Wunut and Watudakon fields were also sampled to conduct dissolved gas analyses (Group 4). Finally, selected rock cuttings from the BJP1-R1 well, originally drilled in the outskirts of the Lusi eruption site (Sutrisna, 2009), were analyzed for the TOC content through the interval 543–884 m of the Pucangan Fm. and 900–993 m of the Up. Kalibeng Fm.

Gas samples were collected in two valve steel and glass samplers. Prior to sampling, the head well was routinely flushed for 20 min to reduce potential contamination of the sample. Bubbling seeps were sampled using a plastic funnel positioned upside-down and connected by silicone tubes to glass or steel tanks. Water was collected in crimped 245-ml glass water flasks.

The analyses of chemical composition of fluids were completed at the Istituto Nazionale di Geofisica e Vulcanologia (INGV-Palermo, Italy). Gas chromatography (GC) was performed using a gas chromatograph (Perkin Elmer Clarus 500) equipped with a double detector (thermal conductivity detector and a flame ionization detector with a methanizer) using Ar as the carrier gas and a 3-m packed column (Restek Shincarbon ST), with analytical errors of <3%.

Dissolved gas samples were extracted by the collected waters and analyzed by using the methodology proposed by Capasso and Inguaggiato (1998).

The carbon isotopic composition of CO_2 ($\delta^{13}C_{CO2}$) was determined using a Thermo Delta XP Isotope Ratio Mass Spectrometer coupled with a Thermo Scientific™ TRACE™ Ultra Gas Chromatograph. Separation prior to analysis was done through a 30-m Q-plot column (i.e., of 0.32 mm). The resulting $\delta^{13}C_{CO2}$ values are expressed in per mil notation with respect to the international Vienna Pee Dee Belemnite (VPDB) standard and analytical uncertainties of ±0.15‰.

The carbon and deuterium isotopic composition of CH_4 ($\delta^{13}C_{CH4}$ and δD_{CH4}) was determined using a Thermo TRACE GC interfaced to a Delta Plus XP gas source mass spectrometer and equipped with a Thermo GC/C III (for Carbon) and with GC/TC peripherals (for Hydrogen). The $^{13}C/^{12}C$ ratios are reported as $\delta^{13}C_{CH4}$ values with respect to the VPDB standard, and $^{2}H/^{1}H$ ratios are reported here as δD_{CH4} values with respect to the Vienna Standard Mean Ocean Water (VSMOW) standard. The analytical uncertainty of the measurements was 0.1‰.

Carbon isotopes of the methane homologs were measured in the Isotech Labs Inc. (Illinois, USA) using three IRMS instruments: Delta Plus, Delta Plus XL, and Delta V Plus.

^{3}He, ^{4}He and ^{20}Ne, and the $^{4}He/^{20}Ne$ ratios were determined by separately injecting He and Ne into a split flight tube mass spectrometer (GVI-Helix SFT, for He analysis) and then into a multicollector mass spectrometer (Thermo-Helix MC plus, for Ne analysis), after standard purification procedures (Correale et al., 2012). The analytical error was generally less than 1%. The R/R_A values were corrected for atmospheric contamination based on the $^{4}He/^{20}Ne$ ratio (Sano & Wakita, 1985). The Ar-isotope composition was measured in a multicollector mass spectrometer (GVI Argus), for which the analytical uncertainty was 0.5%.

Measured He isotopes values are reported as R/R_A, where $R = {}^{3}He/{}^{4}He$, measured in the sample, and $R_A = {}^{3}He/{}^{4}He$ of air (1.4×10^{-6}). Helium concentrations in the analyzed samples range from 5 to 140 ppm. $^{4}He/^{20}Ne$ ratio is 120–1,690 times higher than that measured in air ($^{4}He/^{20}Ne = 0.318$), confirming very low air contamination and validating the accuracy of the results.

Table 1
Major Gas Components of the Sampled Free Gas (Group1-3, in vol.%) and Dissolved Gas (Group 4, in cm3 per Liter at Standard Temperature and Pressure)

Sample ID	Group	Field	Well, sampling depth interval (m)	He	H_2	O_2	N_2	CH_4	CO	H_2S	CO_2	C_2H_6	C_3H_8	$C_1/(C_2+C_3)$
JV17-36	1	Tanggulangin	Well TG5, 742–966	0.0008	nd	0.01	0.7	91.6	nd	nd	4.58	2.66	0.66	28
JV17-37			Well TG1, 468–471	0.0013	nd	0.20	2.1	97.7	nd	nd	0.22	0.14	nd	698
JV17-38			Well TG1SS, 417–425	0.0023	nd	0.11	2.6	96.9	nd	nd	0.06	0.05	nd	1,978
JV17-49			Well TG2, 435–460	0.0026	0.0043	0.16	3.3	96.1	nd	nd	0.08	0.05	nd	2,056
JV17-41		Wunut	Well WU-1ST, 218–246	0.0050	0.0005	1.13	6.9	91.0	nd	nd	0.05	0.03	nd	2,757
JV17-42			Well WU 1A-LS, 341–347	0.0046	0.0002	0.06	2.7	97.2	nd	nd	0.10	0.04	nd	2,745
JV17-50			Well WU9LS, 790–885	0.0005	0.0007	0.25	1.2	96.5	nd	nd	0.37	0.61	nd	158
JV17-39			Well WU16, 627–807 (?573?)	0.0015	0.0008	0.07	1.3	96.3	nd	nd	0.02	1.72	0.42	45
JV17-43		Carat	Well CA-1, 494–500	0.0012	0.0002	0.004	1.2	98.7	nd	nd	0.06	0.06	nd	1,646
JV17-03	2	Surface seep	Bubbling pool	0.0141	0.0043	0.33	7.0	85.2	nd	nd	1.10	3.88	1.60	16
JV17-04			Bubbling pool	0.0139	0.0040	0.28	6.9	83.4	nd	nd	1.18	3.86	1.68	15
JV17-44	3	Watudakon	well WD20, ~350 m	0.0006	0.0011	0.04	0.5	100.0	nd	nd	0.04	0.09	nd	1,118
JV17-46	4	Watudakon	well WD17, ~600 m	0.000426	0.024	0.17	2.33	20.8	0.00204	b.d.l.	8.28	b.d.l.	b.d.l.	
JV18-08		Wunut	well WU15, ~900 m	0.0002	0.00004	3.26	10.5	14.0	b.d.l.	b.d.l.	28.15	b.d.l.	b.d.l.	

Note. nd = not defined, b.d.l. = below detection limit.

TOC measurements were performed on the LECO CS-230, in the Federal Institute for Geosciences and Natural Resources (BGR), Germany. The method is described in Blumenberg et al. (2016).

5. Results

Gas geochemistry results obtained from the sampled localities are summarized in Tables 1 and 2. All sampled gases are methane-dominated (CH_4 > 91.6 vol.%). N_2 is present in variable concentrations (from 0.5 to 7.5 vol.%), and O_2 concentrations are up to 1.13 vol.%. The O_2/N_2 ratio in the collected gases is lower than 0.1 (except the sample JV17-50, 0.21), that is, lower than the same ratio in air (0.27) and in the air saturated water (0.53) showing that these fluids were not affected by strong air contamination.

More specifically, gas samples from the oil and gas production wells around Lusi (Group 1) contain methane ranging from 91 to 99 vol.% and higher methane homologs (ethane < 2.7 vol.% and propane < 0.7 vol.%). The gas dryness ratio $C_1/(C_2+C_3)$ varies from 28 to 2,757 and follows a general trend decreasing with the reservoir depth (Figure 3a). CO_2 concentrations are very low (average value 0.1 vol.%), except for the deepest producing units of TG5 well of Tanggulangin field (4.6 vol.%). The $\delta^{13}C_{CH4}$ varies from −40.7‰ to −58.3‰ and δD_{CH4} from −201‰ to −177‰. The low CO_2 content present in the samples allowed the isotopic measurements to be performed in only two samples from Tanggulangin and Carat fields (18.9‰ and 22.8‰, respectively). He isotopes have a R/R_A ranging between 5.1 and 6.7, with the lowest values recorded in the deepest samples. Ar isotope composition ($^{40/36}$Ar) ranges between 303 and 435, higher than the same ratio in atmosphere (298.6; Ozima & Podosek, 2002).

Two gas samples from the bubbling pools above the Wunut field (Group 2, named surface seep in the Tables 1 and 2) revealed almost identical composition. Together with methane (average 84.3 vol.%) and CO_2 (average 1.14 vol.%), ethane and propane were also detected (3.9 and 1.6 vol.%, respectively). The average gas dryness ratio is 15.3, which is significantly lower than that measured for the Group 1 samples (Figure 3a). The isotopic analyses reveal $\delta^{13}C_{CH4} = -42.5$‰ and ranges of δD_{CH4} from −170‰ to −173‰, $\delta^{13}C_{CO2}$ from 1.2‰ to 2.7‰, and $R/R_A = 6.1$ and $^{40/36}$Ar from 330 to 357.

The gas sampled at the Watudakon gas field (Group 3) is also CH_4-dominated, with ethane abundance <0.09 vol.%. Isotopic analyses revealed $\delta^{13}C_{CH4} = -62.4$‰ and $\delta D_{CH4} = -190$‰, while $\delta^{13}C_{CO2}$ was not measured due to low CO_2 concentration (599 ppm).

Table 2
Isotopic Composition of the Sampled Free Gas

Sample ID	Group	Field	$\delta^{13}C_{C1}$	$\delta^{13}C_{C2}$	$\delta^{13}C_{C3}$	$\delta^{13}Ci_{C4}$	$\delta^{13}Cn_{C4}$	$\delta^{13}Ci_{C5}$	$\delta^{13}Cn_{C5}$	$\delta^{13}C_{CO2}$	δD_{CH4}	R/ R_A	He	Ne	$^4He/^{20}Ne$	R/Ra $_c$	$^{40}Ar/^{36}Ar$	^{40}Ar
JV17-36	1	Tanggulangin	−40.7	−25.7	−16.6	−22.6	−19.3	−21.8	−18.4	18.9	−181.5	5.9	7.3	0.04	194.3	5.9	435.0	18.7
JV17-37			−50.7								−200.9	5.9	13.8	0.09	147.6	5.9	323.2	83.8
JV17-38			−57.1								−196.9	6.6	22.7	0.17	130.1	6.6	308.9	181.1
JV17-49			−58.3								−198.4	6.2	25.4	0.66	38.4	6.2	303.4	288.9
JV17-41		Wunut	−48.5								−197.3	6.3	50.3	0.09	537.4	6.3	345.2	142.6
JV17-42			−47.8								−195.1	6.3	45.2	0.09	492.0	6.3	368.6	99.1
JV17-50			−57.7								−190.6	5.1	4.6	0.09	51.6	5.1	307.0	36.5
JV17-39			−41.8	−23.4	−16.1	−21.8	−18.1	−20.8			−176.8	5.9	14.9	0.18	81.6	5.9	357.0	40.6
JV17-43		Carat	−41.4							22.8	−195.6	6.7	11.2	0.03	371.4	6.7	313.8	84.3
JV17-03	2	Surface seep	−42.6	−27.1	−24.5	−25.7	−23.2	−23.8	−21.6	2.7	−170.4	6.1	143.1	0.46	313.5	6.2	357.3	326.3
JV17-04			−42.5							1.2	−173.3	6.1	142.7	0.92	155.5	6.1	329.5	563.5
JV17-44	3	Watudakon	−62.4	−30.8							−190.1	2.1	5.8	0.10	56.5	2.1	300.5	83.1

Note. Isotopic data: $\delta^{13}C$ (‰VPDB); δD (‰VSMOW); $R/R_A = (^3He/^4He)$ sample/ $(^3He/^4He)$ atmosphere. He, Ne, and ^{40}Ar concentrations in parts per million.

The measurements of water-dissolved gases of the Watudakon gas field (Group 4) are CH_4-dominated (20.8-cm^3/l Standard Temperature and Pressure (STP); Table 1) but with also high content of CO_2 (up to 8.28 cm^3/l STP). This last value is 27 times higher than that measured in the Air Saturated Waters values (ASW = 0.31 cm^3/l STP). Helium isotope composition revealed R/R_A = 2.14 and $^{40/36}Ar$ equals to 300.5‰. Water-dissolved gases at the Wunut field (Group 4) are CO_2-dominated (28.15 cm^3/l STP, Table 1) with CH_4 content of 13.97 cm^3/l STP.

Measured TOC in the cuttings of the Pucangan and Upper Kalibeng Formations from the BJP-R1 well resulted in 0.5 to 1.75 wt.% (average 0.9 wt.%).

6. Discussion

The acquired geochemical data set allowed to identify the origin of the gases that are trapped in the shallow HC reservoirs produced in the northeast Java. Furthermore, we combined the data in order to investigate if a possible connection exists between the neighboring Arjuno-Welirang volcanic complex and the reservoirs. This is described in detail in the following sections.

6.1. HC Origin and Alteration Processes in the Reservoirs

The origin of natural gases, trapped in the porous media, is commonly characterized using binary genetic diagrams of $\delta^{13}C_{CH4}$ versus δD_{CH4}, $\delta^{13}C_{CH4}$ versus $C_1/(C_2 + C_3)$, and $\delta^{13}C_{CH4}$ versus $\delta^{13}C_{CO2}$. These empirical diagrams were first proposed in 1970s–1980s (Bernard et al., 1977; Gutsalo & Plotnikov, 1981; Schoell, 1983; Whiticar et al., 1986) and have been more recently revised based on >690,000 data entries (Milkov & Etiope, 2018). This recent study highlights that the original molecular and isotopic composition of CH_4, its homologs, and CO_2 could be affected by several post-generation processes, including mixing, migration, biodegradation, thermochemical sulfate reduction, and oxidation. Therefore, a combined use of these plots is required to obtain distinctive conclusions in order to classify gases in natural systems.

Methane isotope composition of the gas from Group 1 ($\delta^{13}C_{CH4}$ range from −58.3‰ to −40.7‰ and δD_{CH4} from −201‰ to −170‰) coupled to the ratio $C_1/(C_2 + C_3)$ indicates that the studied natural gases have mainly thermogenic origin (i.e., generated within organic-rich sediments due to thermal cracking of the kerogen), even if CH_4 from different reservoirs of the Group 1 shows a large variability of its isotopic composition (Figures 3b and 3c). These results are consistent with the migration of HCs from the organic-rich deep sited (>4 km) Middle Eocene-Lower Oligocene Ngimbang source rock (Kusumastuti et al., 1999). The HCs were presumably initially trapped in the Miocene reef carbonates of the Porong structure (located few kilometers to the east from the studied HC fields; see Figure 1b for location). After the collapse of the seal above this carbonate reservoir, HCs migrated through a system of faults to the shallow porous units of the Pucangan Fm during the Late Pleistocene-Holocene and migrated toward the west in the targeted reservoirs (Kusumastuti et al., 1999).

The positive carbon isotope ratio of the CO_2 ($\delta^{13}C_{CO2}$ +18.9‰ and +22.8‰) indicates that the HC reservoirs are affected by biodegradation processes (Figure 3d). Biodegradation is commonly taking place in

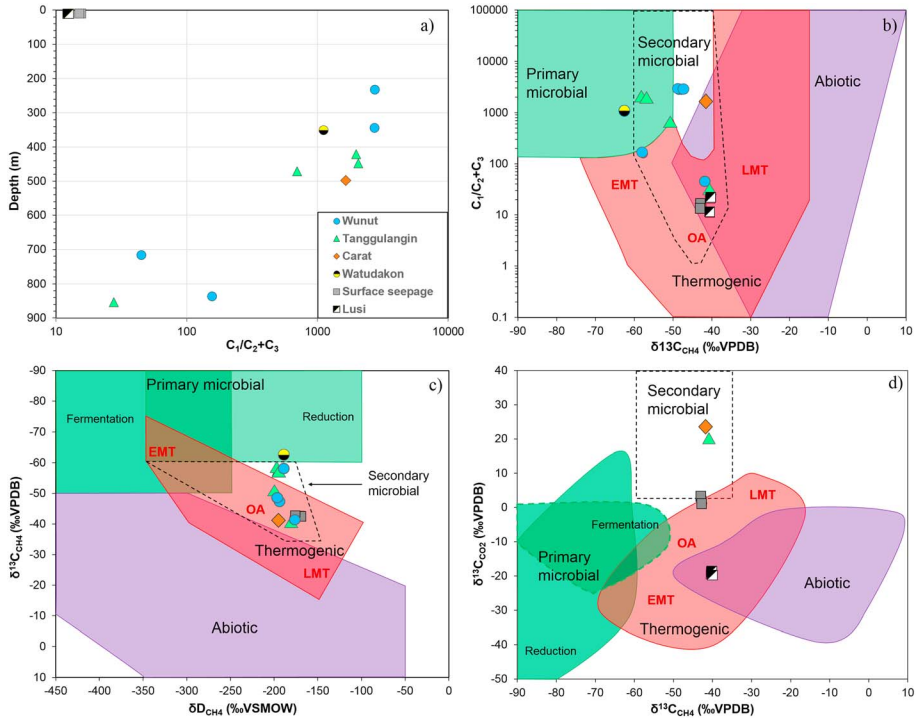

Figure 3. (a) The dryness plot of the sampled HC gases versus the reservoir depth reveals decreasing values at higher depths. The gas erupted at the Lusi surface, and adjacent seepages is wet. Gas genetic diagrams of (b) $C_1/(C_2 + C_3)$ versus $\delta^{13}C_{CH4}$; (c) $\delta^{13}C_{CH4}$ versus δD_{CH4}; (d) $\delta^{13}C_{CO2}$ versus $\delta^{13}C_{CH4}$; after Milkov and Etiope (2018). The genetic diagrams reveal the thermogenic origin of the gas sampled from the shallow HC reservoirs at Wunut, Tanggulangin, and Carat fields (Group 1) and the surface seepages (Group 2). The gas composition is altered by biodegradation processes, therefore mixed with secondary microbial gas. The gas sampled from the Watudakon field is of primary microbial origin. The majority of the sampled HC gas from the reservoirs is dry. HC gas from the Lusi crater (Mazzini et al., 2012), surface seepages, and two HC reservoirs (this study) is wet. EMT = Early Mature Thermogenic gas; LMT = Late Mature Thermogenic gas; OA = oil-associated gas; HC = hydrocarbon.

shallow HC reservoirs at temperatures below 80–90 °C (Head et al., 2003; Milkov, 2010, and references therein) and can be simplified in two main steps: 1) anaerobic oxidation of the thermogenic HCs followed by microbial CO_2 production, combined with (2) microbial (operated by methanogens) CH_4 generation via CO_2 reduction (Etiope et al., 2009; Milkov, 2018). Due to preferential selection by the methanogens of the ^{13}C-depleted CO_2, the residue CO_2 is enriched in ^{13}C carbon isotope (Head et al., 2003; Milkov, 2011). Occurrence of biodegradation process in the reservoirs is also supported by the available carbon isotope analyses of the methane homologs (C_nH_{2n+2}) in the studied samples. The $\delta^{13}C$ measured on gaseous HCs formed due to thermocracking processes of, typically follows a regression trend (i.e., $\delta^{13}C_{CH4} < \delta^{13}C_{C2H6} < \delta^{13}C_{C3H8} < \delta^{13}C_{C4H10}$, Chung et al., 1988; Schoell, 1983). An irregular trend is instead present in reservoirs with T < 80–90 °C affected by the HC biodegradation processes. This process occurs because of the selective preference of bacteria to use some homologs over others, that is propane and n-butane over ethane and isobutane (Wenger et al., 2002). Similarly to CO_2 microbial consumption, the bacteria favor the ^{13}C-depleted C_nH_{2n+2}, that is controlled by the bacterial enzymatic processes and C-C bond energies (Peters et al., 2005). As a result, the remaining C_nH_{2n+2} molecules are enriched in ^{13}C carbon. Our analyses, and the one described in Mazzini et al. (2012), reveal that the observed carbon isotope ratios trend (Figure 4) are consistent with the biodegradation processes described above.

A potential contribution of methane generated within the shales of the Pucangan and/or Kalibeng Formations cannot be excluded; however, this should be a limited amount given the relatively low TOC in this formation (TOC from 0.5 to 1.75 wt.%, average 0.9 wt.%).

The natural gas sampled at the Watudakon field is essentially methane-dominated with a clear microbial isotopic signature ($\delta^{13}C_{CH4}$ and δD_{CH4} are −62.4‰ and −190.1‰, respectively; Figures 3b and 3c). This

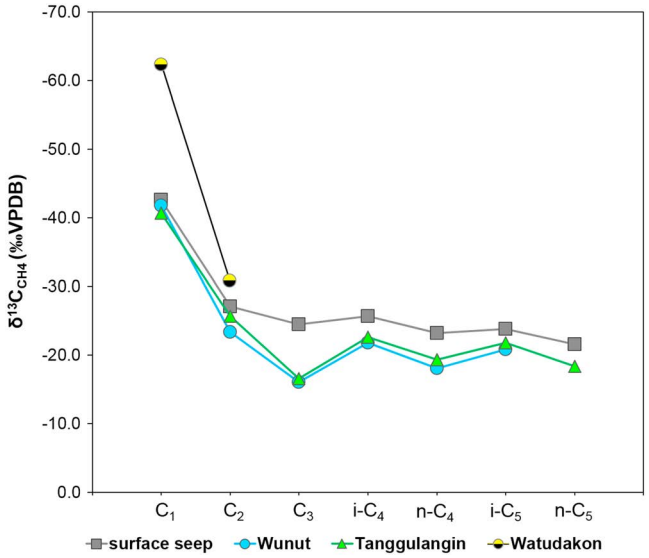

Figure 4. Carbon isotope distribution of the methane homologues in the samples from the Tanggulangin, Wunut, and Watudakon fields and surface seep. The plot indicates the occurrence of the hydrocarbon biodegradation processes in the Tanggulangin and Wunut reservoirs. Gas sampled at the surface seep above the Wunut field does not show the evidence of significant biodegradation.

indicates either (1) biodegradation processes of thermogenic HCs (gaseous and liquid), earlier generated by thermocracking process, or (2) ongoing microbial methanogenesis in the shallow organic-rich clays that interbed the porous media hosting the gas. According to the well log data from the Watudakon 20 well, there is no record of oil shows or other oil traces in the well. The trace amount of C_{2+} gases (lower than 0.1%) also supports a primary microbial origin of the methane. These data may suggest that the migration of HCs from the Ngimbang source rock did not occur in this peripheral part of the basin and that more recent microbial processes are currently very active.

6.2. Migration of the Mantle-Derived Fluids in the Sedimentary Basin

He isotopes represent a powerful tool for recognizing the occurrence of mantle-derived fluids in sedimentary HC reservoirs and in continental region away from volcanism (e.g., O'Nions & Oxburgh, 1988; Prinzhofer, 2013). He is an inert gas, highly mobile, physically stable, it has two stable isotopes (^{3}He and ^{4}He), and their isotopic signatures in the pristine reservoirs (atmosphere, crust and mantle) are strongly different: ^{3}He has a primordial origin and is usually degassed from the mantle (Ozima & Podosek, 2002); ^{4}He is produced by U and Th decay. Three major He reservoirs have distinct ^{3}He/^{4}He isotope ratios: (1) crust 0.01 R_A ($R_A = {}^3\text{He}/{}^4\text{He}$ of air, 1.4×10^{-6}); (2) atmosphere 1 R_A; and (3) mantle from ~8 ± 1 R_A (Mid-Ocean Ridge Basalts mantle reservoir; Ozima & Podosek, 2002).

Our results (Table 2) reveal that all the samples from the HC reservoirs have a high ^{3}He/^{4}He isotope ratios (R/R_A as high as 6.7). Argon isotope composition ($^{40/36}$Ar) in the collected fluids shows that these fluids have low air contamination. This is confirmed by the values of the ^{4}He/^{20}Ne ratios that are higher than the same ratio in the atmosphere ($^4\text{He}/^{20}\text{Ne}_{AIR} = 0.318$, Table 2).

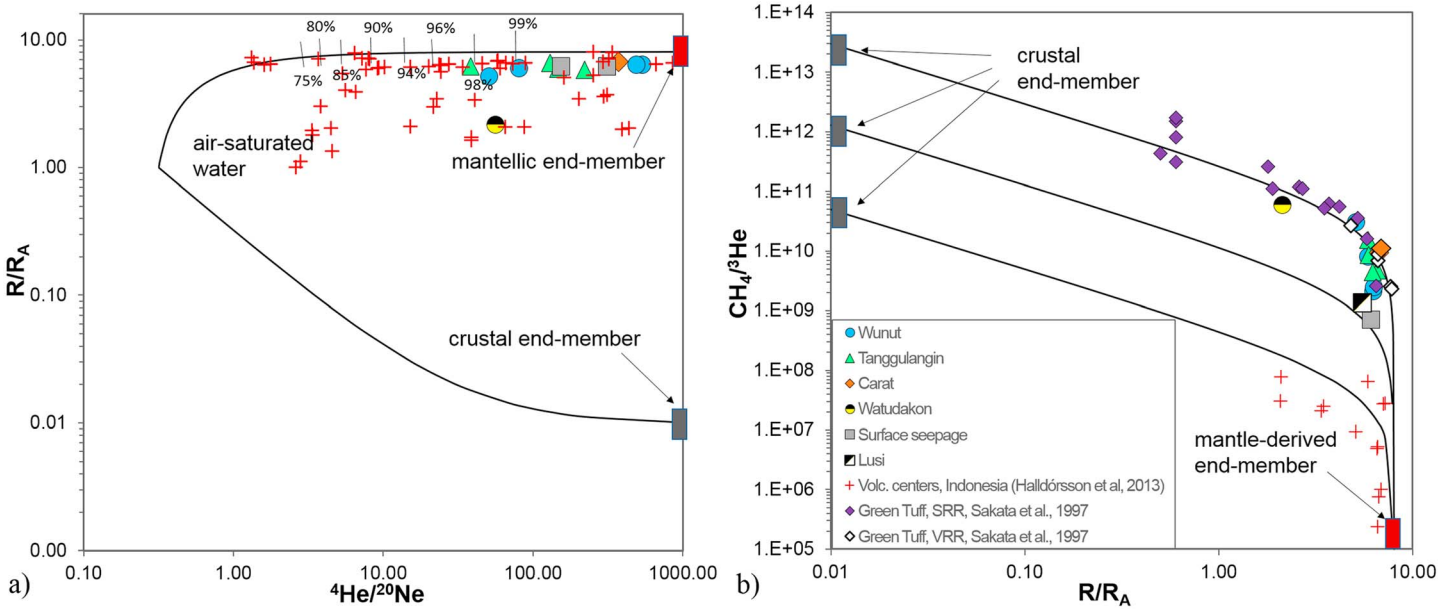

Figure 5. (a) Plot of the measured He isotopes versus ^{4}He/^{20}Ne ratio showing the integrity of the He isotope results. The curves represent mixing between air-saturated water (1 R_A), Mid-Ocean Ridge Basalts (8 R_A), and crust (0.01 R_A); (b) plot of the $CH_4/^3$He ratio versus He isotopes (R/R_A). Black lines indicate two-component mixing of the mantle-derived end-member ($CH_4/^3\text{He} = 1.0 \times 10^5$ and ^{3}He/^{4}He = 8 R_A) and crustal end-member with three possible compositions ($CH_4/^3\text{He} = 5.0 \times 10^{10}$, 1.3×10^{12}, and 3.0×10^{13} with a common ^{3}He/^{4}He = 0.01 R_A), adopted after Halldórsson et al. (2013) and Jenden et al. (1993). The plot demonstrates that even in the systems with high CH_4 abundance, He could have low crustal contamination.

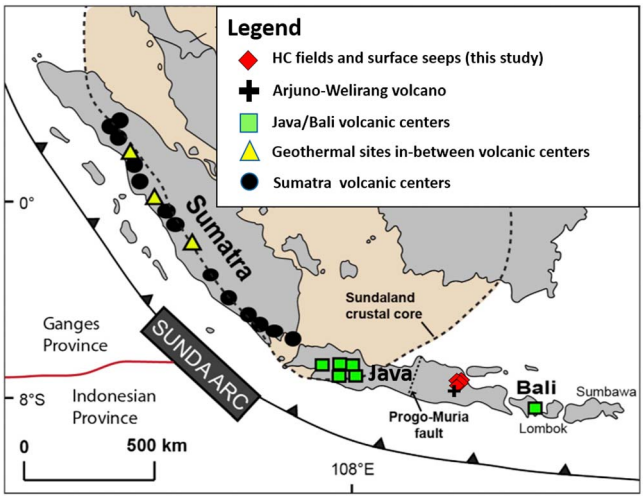

Figure 6. Map of Indonesia, modified after Halldórsson et al. (2013), showing measured He isotopes distribution through the Sunda arc (Halldórsson et al., 2013), at the Arjuno-Welirang volcano (Inguaggiato et al., 2018), and in the southern part of the East Java sedimentary basin (this study, red diamonds). HC = hydrocarbon.

The ranges of the measured He-isotope compositions and $^4He/^{20}Ne$ ratios in the collected gases can be explained in terms of mixing between three sources of He (Sano et al., 1997): atmosphere, mantle, and crust (Figure 5a). Since the investigated systems are located in a continental region, we assumed a Mid-Ocean Ridge Basalts mantle source in the area with a He-isotope ratio of 8 ± 1 Ra, as suggested by Halldórsson et al. (2013). We then computed the contributions of atmospheric, radiogenic, and mantle-derived He on the basis of the analytical $^3He/^4He$ and $^4He/^{20}Ne$ ratios (Sano et al., 1997). The fluids associated with the investigated HCs contain mantle He contributions from ~98% to ~99.9% (Figure 5a).

In order to constrain the possible origin of CH_4 in the HC reservoirs, we used the approach proposed by Poreda et al. (1988) that is based on a two component crust-mantle mixing model, $CH_4/^3He$ ratios versus He isotopes (Figure 5b). We used three possible crustal end-members with $CH_4/^3He = 5.0 \times 10^{10}$, 1.3×10^{12}, and 3.0×10^{13}, with common $^3He/^4He = 0.01\ R_A$, and a mantle-derived end-member with $CH_4/^3He = 1 \times 10^5$ and $^3He/^4He = 8\ R_A$ (Halldórsson et al., 2013). The proposed mixing model reveals that crustal end-member with $CH_4/^3He = 3.0 \times 10^{13}$ is the most suitable for our data set. Although the investigated reservoirs are methane-dominated, the measured $CH_4/^3He$ ratios are similar to those in the geothermal systems of subduction zones (Snyder et al., 2003, and references therein) and those measured in the volcanic rock reservoirs of natural gas fields in the Green Tuff basin, Japan (Sakata et al., 1997; Figure 5b). However, $CH_4/^3He$ ratio in the HC reservoirs is 2 to 3 orders of magnitude higher than in the volcanic centers along the western Sunda Arc (Halldórsson et al., 2013). These findings confirm the presence of a specific setting where methane-dominated reservoirs are heavily affected by the migration of mantle-derived He. This situation presents new questions and scenarios regarding the migration of magmatic fluids that are typically CO_2-dominated.

6.3. Noble Gas Distribution Through the Sunda Arc

Our data fit well with those from previous investigations in natural fluids emitted in volcanic and hydrothermal systems in the western and central Sunda Arc (Halldórsson et al., 2013), where the outgassing volatiles are dominated by CO_2. Here the majority of the He isotopes ratios range from 5.3 to 8.1 R_A (Figure 6). Hence, at regional scale, the mantle wedge is considered to be the principal source of He at volcanic centers. However, a minor radiogenic contamination from the subducted crust can also be inferred, particularly in the western part of the Sunda Arc, where thicker and older crust is present, decreasing the typical mantle-derived He signature in the emitted volatiles. However, the large database described by Halldórsson et al. (2013) contains a gap in the central and eastern part of Java. Our novel data together with the He data from the Arjuno-Welirang volcanic system (Inguaggiato et al., 2018) and those from the Lusi crater (Mazzini et al., 2012) contribute to the filling of this gap and to the reconstruction of the general distribution of the magmatic volatile sources along the eastern Sunda Arc. Furthermore, our results demonstrate a propagation of the mantle-derived volatiles from the volcanic complex to the sedimentary basin around the Lusi system.

6.4. The Fate of Magmatic CO_2

CO_2, CH_4, and H_2O are considered as the main He carriers for migration through the crust in sedimentary and volcanic settings. Previous results and modeling indicate that CO_2 is the major magmatic volatile migrating through the East Java Basin, particularly at and around the Lusi eruption site (Mazzini et al., 2012; Sciarra et al., 2018; Svensen et al., 2018; Vanderkluysen et al., 2014). Therefore, in our study case, CO_2 is assumed to be the carrier for the migration of the mantle-derived He in the sedimentary basin and the HC reservoirs. Nevertheless, the gas sampled in the HC reservoirs (Group 1) reveals very low CO_2 concentrations, varying from 0.02 to 0.37 vol.% (except for the well TG5), and concurrently high R/R_A values (Tables 1 and 2). Furthermore, the carbon isotopic composition of CO_2 is extremely positive (from +18.9‰ to +22.8‰) and significantly different from the typical composition of the mantle-derived CO_2

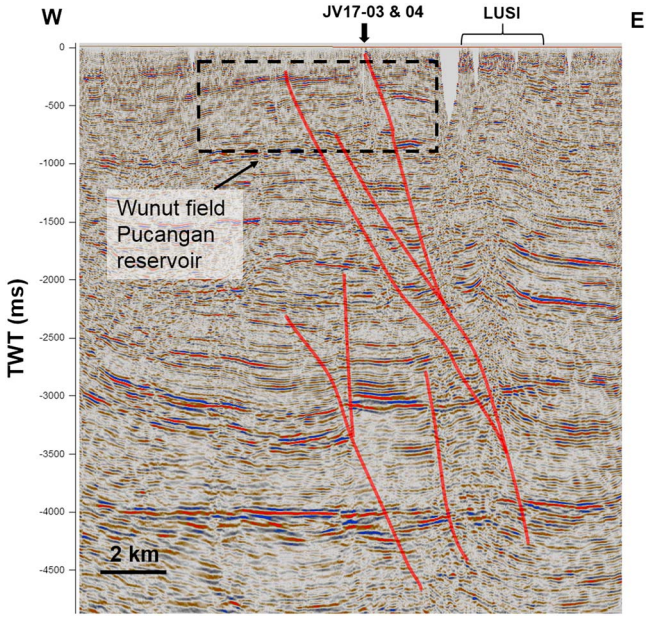

Figure 7. W-E-oriented seismic profile from 2003, with indicated location of the sampled surface seepage site, Lusi, the conditional location of the shallow hydrocarbon reservoirs of the Wunut field and several faults as part of the Watukosek Fault System (highlighted in red). Faults act as migration pathway for the fluids. Profile location indicated in Figure 1b. TWT represents two-way travel time.

($-8‰ < \delta^{13}C_{CO2} < -4‰$; Clark & Fritz, 1997; Deines, 2002). Hence, mantle-derived CO_2 seems to be decoupled from the mantle-derived He. There are two potential mechanisms able to mask the CO_2 as carrier gas: (1) CO_2 transformation to CH_4 by microbial activity and (2) CO_2 dissolution in the water. The first hypothesis is that large part of the CO_2 is transformed by microbial activity operated by methanogens (as described in the section 6.1). An additional hypothesis is that during the migration of mantle-derived He and CO_2, the latter gets mainly dissolved in formation water. This process is able to reduce the amount of CO_2 in the gas phase and preserve the pristine isotopic ratio of He that does not dissolve into water (Caracausi et al., 2003). This mechanism is not applicable for ongoing focused and vigorous seepage. For example, deep and hot CO_2-rich fluids at Lusi are flushed rapidly toward the surface without cooling. When instead diffused fluids migration occurs at slower rates through gradually colder sedimentary rock formations, the dissolution of CO_2 takes place. Furthermore, it is recognized that the transport of He could be decoupled from that of carbon gases in the areas away from the active volcanism (Giggenbach et al., 1993). The depicted scenario is further supported by the significant concentration of dissolved CO_2 in the water (8.28 and 28.15 cm^3/l STP at the Watudakon and Wunut fields, respectively, Group 4). Here the amount of the dissolved CO_2 is higher than in the water in equilibrium with the atmosphere (0.31 cm^3 SPT/l; Capasso & Inguaggiato, 1998), indicating that part of CO_2 can be dissolved in the shallow formation waters.

6.5. The Subsurface Plumbing System

To investigate potential fluid migration pathways, we compared the fluid geochemistry at different sites and complemented these data with available subsurface geophysical data. Gas compositions of the fluids emitted at the surface seepage sites above the Wunut reservoir (Group 2) are distinctively different from those recorded at the adjacent WU1 well (Tables 1 and 2). However, the origin of the HC gases is always thermogenic ($\delta^{13}C_{CH4}$ as high as $-42.5‰$ and δD_{CH4} as high as 170.4‰ $C_1/(C_2 - C_3) = 15$; Table 2 and Figures 3b and 3c). Furthermore, these seeps contain 5–10 times more CO_2 than samples of Group 1 (where CO_2 is almost absent) with a different isotopic signature (i.e., $\delta^{13}C_{CO2}$ between 1.2‰ and 2.7‰). These marked differences suggest that a diverse source of fluids is present at this locality or that some processes (i.e., mixing) may occur during the transfer of the fluids toward the surface.

Insights about the subsurface plumbing system are provided by seismic profiles acquired during the 1990–2000s in this part of the basin. Geophysical data highlight the occurrence of the WFS that extends from the Arjuno-Welirang volcanic complex, intersects Lusi, and progresses toward the northeast Java (Moscariello et al., 2018). The authors describe the presence of this deep-rooted fault system that splits laterally at shallower depths and creates a network of fractures. These faults either stop within the topmost kilometer of sediments or can be traced all the way to the surface. This type of features can also be observed on the seismic lines crossing the Wunut field, sampled seepage zone (Group 2), and Lusi (Figure 7). Here one of these faults reaches the surface exactly at the Group 2 seepages locality. Additional faults can also be observed ending below, and sometimes within, the Wunut field. Therefore, these fractured zones represent ideal pathways for the transfer of fluids due to their high permeability within the reservoir and at the surface.

An additional fluids source that is feeding the surface seeps at the Wunut locality (Group 2) is potentially provided through broad caldera collapse and diffused fracturing ongoing around the neighboring Lusi crater, located 3.5 km to the east (Mauri et al., 2018; Panzera et al., 2018). These newborn fractures represent additional active pathways for radial transfer of the Lusi fluids in the shallow surface. Here thousands of active seeps are scattered around the Lusi vent and have CO_2 and CH_4 signatures similar to those measured for Group 2 (Tables 1 and 2; Mazzini et al., 2012; Sciarra et al., 2018). Further, the authors also describe the presence of ~W-E-oriented systems of newborn antithetic fractures that are interpreted to result from the sinistral strike-slip activity of the WFS. These fractures, similarly to the NE-SW-oriented WFS, are proven

to be an active advective pathway for the migration of fluids (Sciarra et al., 2018). Gravimetry data (Mauri et al., 2018) also confirm the presence of these structures that are likely recycled by the radial fluids expulsion from the over pressured Lusi conduit.

6.6. HC Reservoirs, Lusi, and the Volcanic System

Our results indicate that mantle-derived fluids not only migrate from the volcanic complex at focused localities such as the Lusi site (Inguaggiato et al., 2018; Mazzini et al., 2012) but also disperse over a broader area within the sedimentary basin through which the WFS extends. The highest He isotope signature was measured in the fluids trapped in the Carat field (6.7 R_A), the closest field to the volcanic complex. (Figures 1b and 2). In contrast, the lowest He isotope ratio was distinguished in the Watudakon field (2.1 R_A), located on the outskirts of the magmatic complex (Figures 1b and 2) but in a part of the basin that is not intersected by the WFS (i.e. ~36 km west of Lusi). This lower He isotope signature indicates that here the crustal He component (^{4}He due to U and Th decay in the crust) is higher (Figures 5a and 5b). The migration pathway of the mantle-derived volatiles toward the Watudakon field is less developed than the one existing for the fields located along the WFS. It is worth noting that the Watudakon field also has a different CH_4 signature indicated as primary microbial origin (Figures 3b and 3c). Hence, this reservoir contains volatiles that are very distinct with respect to those in the Wunut, Tanggulangin, and Carat reservoirs. This observation strengthens the hypothesis that the migration of mantle-derived fluids mainly occurs in the region around the volcanoes but that enhanced migration is promoted in the NE-SW-oriented corridor crossed by the WFS. This observation is also consistent with the thermal gradient measured from these fields based on the available shallow boreholes. The data indicate a gradient of 2.8–4.8 °C/100 m from Wunut field, 3.8–4.8 °C/100 m from Tanggulangin, and 4.9 °C/100 m from Carat. These values are remarkably similar to the gradient measured at the BJP-1 well (4.2 °C/100 m; Mazzini et al., 2007) drilled prior to the occurrence of the Lusi eruption. The evidence of a widespread high thermal gradient is in agreement with the broadly diffused migration of mantle-derived fluids.

Our new data also help to refine the fluids migration imaged by the ambient noise tomography acquired in the region that indicates the migration of hydrothermal fluids from the volcanic arc toward the sedimentary basin (Fallahi et al., 2017). The major migration pathway is linked to the WFS as well as W-E-oriented systems of antithetic fractures present around Lusi. Considering the remarkable variation of the geochemical composition of the C-rich gases (i.e., CO_2 and CH_4) sampled from the HC fields (this study) and the Lusi system (Mazzini et al., 2012), we can conclude that these two systems are essentially compartmentalized and input of fluids from the Lusi system to reservoirs is limited. The slow migration of mantle-derived He in the HC reservoirs occurs independently from the focused one occurring at the Lusi crater. We cannot rule out the possibility that fluids (i.e., CO_2 and CH_4) outgassing from the Lusi system may also move laterally toward the HC reservoirs (Wunut, Carat, and Tanggulangin) and are later modified by secondary processes (i.e., biodegradation). However, the collected data do not support this scenario.

6.7. Basinal Fluids Migration

Based on the findings and observations reported herein, merged with the known regional studies, we have developed a schematic model describing the fluids migration in the studied petroleum system (Figure 8).

1. *Deposition of petroleum system elements:* (a) Ngimbang Fm. HC source rock; (b) reservoir (volcaniclastic sands and sandstones); and (c) seals (intercalating shales) both within the Pucangan Fm. HC generation within the Ngimbang Fm., offshore northeast Java.
2. Late Pleistocene-Holocene HC fluid *migration to shallow reservoirs* of the Pucangan Fm., following the collapse of the Porong trap (7 km to the east).
3. *Alteration* of the gas and oil via HC biodegradation process.
4. *Magmatic and hydrothermal fluids migration* toward the organic-rich shales of the deep-seated Ngimbang Fm. (>3,800-m depth) generated additional HCs and CO_2, creating overpressure within the Ngimbang Fm., enriching the gas with mantle-derived trace noble gases (^{3}He and ^{36}Ar).
5. These fluids migrated toward the surface through fractured and weak zones and are present today in the producing HC reservoirs and at the Lusi eruption site.

The gas geochemistry survey described herein corroborates all the previously collected geophysical, petrographic, geochemical, and modeling evidences (Collignon et al., 2018; Fallahi et al., 2017; Malvoisin et al.,

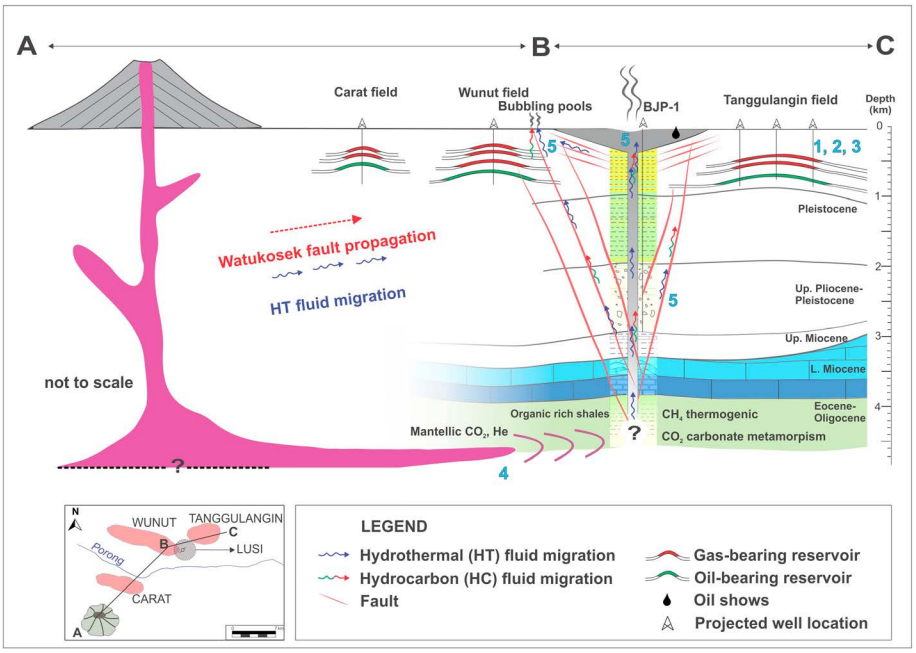

Figure 8. Conceptual geological model depicting the development of the petroleum system and the migration pathways of the mantle-derived and HC fluids in the study area. The major events are marked with Numbers 1–5, described in the section 6.7.

2018; Mazzini et al., 2012; Mazzini et al., 2018; Samankassou et al., 2018; Svensen et al., 2018). These converging data indicate that prior to the Lusi eruption and prior to the drilling of the BJP-1 well, an overpressured zone in the deeply buried Ngimbang Fm. (>4 km) already existed. Here the migration of magma and hydrothermal fluids from the neighboring volcanic arc generated significant overpressure confined in this proliferous source rock buried more than 1 km below the bottom of the BJP-1 well. Therefore, the presence of this naturally overpressured system and its final manifestation at the surface appear to be unrelated to the drilling of the BJP-1 well.

7. Conclusions

We report the results of a gas geochemistry survey conducted in the southern part of the East Java sedimentary basin. Here several HC fields and adjacent surface seepage sites are located near the Arjuno-Welirang volcanic complex and around the Lusi eruption site. The samples collected from the shallow (200–1,000 m) HC fields (Group 1) reveal the presence of predominantly dry thermogenic gas ($-58.3 < \delta^{13}C_{CH4} < -40.7$). Ongoing biodegradation processes are confirmed by the CO_2 signature with $+18.9 < \delta^{13}C_{CO2} < +22.8$. The surface seepages (Group 2) located above the reservoirs reveal a remarkably different geochemical signature where less molecularly and isotopically fractionated and recently generated thermogenic gas is mixed with CO_2 with $+1.2 < \delta^{13}C_{CO2} < +2.7$. All the analyzed samples reveal the presence of noble gases with a clear mantle-derived He signature that is comparable to that in the fluids emitted at the Lusi and Arjuno-Welirang fumaroles. Only a moderate decrease in $^3He/^4He$ ratio is observed along a NE-oriented transect from the Arjuno-Welirang fumaroles ($R = 7.3\ R_A$), through the neighboring Carat HC reservoir ($R = 6.7\ R_A$), Lusi (R up to $6.5\ R_A$), and the surrounding HC fields that still display remarkably high values (R up to $6.3\ R_A$).

The study region is intersected by the WFS that originates from the Arjuno-Welirang volcanic complex, hosting Lusi and the sampled HC fields. Previous studies revealed that this fault system provided the pathway for the magmatic fluids fueling the Lusi eruption. Our new results show that this system of faults also allows the ongoing migration of mantle-derived fluids over a larger region of the sedimentary basin hosting the HC fields. Potential migration of the shallow Lusi fluids to the reservoirs followed by alteration processes (i.e., biodegradation) cannot be totally excluded. However, the distinct signature of the C gases (i.e., CO_2 and

CH_4) observed at the Lusi eruption site and in the HC fields indicates that this input should be limited. Additional fluids expelled at the thousands of seeps around the Lusi crater (including those from Group 2) are migrating from the Lusi conduit through a network of fractures antithetic to the Watukosek strike slip fault system and through the caldera collapse shallow fractures that extend over kilometers around the main Lusi vent.

This study highlights that continuous monitoring of noble gas composition in HC fields neighboring volcanic centers could represent an efficient and logistically simple tool to distinguish perturbations of adjacent magmatic complexes.

Acknowledgments
The work was funded by the European Research Council under the European Union's Seventh Framework Programme Grant agreement 308126 (LUSI LAB project, A. Mazzini). We acknowledge the support from the Research Council of Norway through its Centres of Excellence funding scheme, Project 223272 (CEED). The authors would like to thank the management of Lapindo Brantas Indonesia and PT. Kimia Farma for providing access to the subsurface data and for the authorization to publish the results of this study. BPLS is thanked for their support during the field operations. Federal Institute for Geosciences and Natural Resources (BGR) is thanked for helping with TOC measurements. The interpretation and model presented in this paper reflect solely the view of the authors at the stage of the manuscript preparation. We are grateful to the Editor and two Reviewers who made insightful comments and contributed to improve the quality of the manuscript. The data supporting the paper is represented in the Tables 1 and stored at the NIRD database (https://archive.sigma2.no/pages/public/datasetDetail.jsf?id=C9898994-C249-4190-84B4-13334E9E7B59).

References

Bernard, B., J. M. Brooks, and W. M. Sackett (1977), A geochemical model for characterization of hydrocarbon gas sources in marine sediments, paper presented at 9th Annual OTC Conference.

Blumenberg, M., Lutz, R., Schlömer, S., Krüger, M., Scheeder, G., Berglar, K., et al. (2016). Hydrocarbons from near-surface sediments of the Barents Sea north of Svalbard—Indication of subsurface hydrocarbon generation? *Marine and Petroleum Geology*, *76*, 432–443. https://doi.org/10.1016/j.marpetgeo.2016.05.031

Capasso, G., & Inguaggiato, S. (1998). A simple method for the determination of dissolved gases in natural waters. An application to thermal waters from Vulcano Island. *Applied Geochemistry*, *13*(5), 631–642. https://doi.org/10.1016/S0883-2927(97)00109-1

Caracausi, A., Italiano, F., Paonita, A., Rizzo, A., & Nuccio, P. M. (2003). Evidence of deep magma degassing and ascent by geochemistry of peripheral gas emissions at Mount Etna (Italy): Assessment of the magmatic reservoir pressure. *Journal of Geophysical Research*, *108*(B10), 2463. https://doi.org/10.1029/2002JB002095

Caracausi, A., Paternoster, M., & Nuccio, P. M. (2015). Mantle CO_2 degassing at Mt. Vulture volcano (Italy): Relationship between CO_2 outgassing of volcanoes and the time of their last eruption. *Earth and Planetary Science Letters*, *411*, 268–280. https://doi.org/10.1016/j.epsl.2014.11.049

Caracausi, A., & Sulli, A. (2019). Outgassing of mantle volatiles in compressional tectonic regime away from volcanism: The role of continental delamination. *Geochemistry, Geophysics, Geosystems*, *20*, 2007–2020. https://doi.org/10.1029/2018GC008046

Chung, H. M., Gormly, J. R., & Squires, R. M. (1988). Origin of gaseous hydrocarbons in subsurface environments: Theoretical considerations of carbon isotope distribution. *Chemical Geology*, *71*(1-3), 97–104. https://doi.org/10.1016/0009-2541(88)90108-8

Clark, I., & Fritz, P. (1997). *Environmental isotopes in hydrogeology*. Boca Raton, FL: CRC Press/Lewis Publishers.

Collignon, M., Mazzini, A., Schmid, D. W., & Lupi, M. (2018). Modelling fluid flow in active clastic piercements: Challenges and approaches. *Marine and Petroleum Geology*, *90*, 157–172. https://doi.org/10.1016/j.marpetgeo.2017.09.033

Correale, A., Martelli, M., Paonita, A., Rizzo, A., Brusca, L., & Scribano, V. (2012). New evidence of mantle heterogeneity beneath the Hyblean Plateau (southeast Sicily, Italy) as inferred from noble gases and geochemistry of ultramafic xenoliths. *Lithos*, *132-133*, 70–81. https://doi.org/10.1016/j.lithos.2011.11.007

Deines, P. (2002). The carbon isotope geochemistry of mantle xenoliths. *Earth-Science Reviews*, *58*(3-4), 247–278. https://doi.org/10.1016/S0012-8252(02)00064-8

Devi, E. A., Rachman, F., Satyana, A. H., Fahrudin, F., & Setyawan, R. (2018). Paleofacies of Eocene Lower Ngimbang source rocks in Cepu Area, East Java Basin based on biomarkers and carbon-13 isotopes. *IOP Conference Series: Earth and Environmental Science*, *118*, 012009. https://doi.org/10.1088/1755-1315/118/1/012009

Doust, H., & Noble, R. A. (2008). Petroleum systems of Indonesia. *Marine and Petroleum Geology*, *25*, 103–129. https://doi.org/10.1016/j.marpetgeo.2007.05.007

Etiope, G., Feyzullayev, A., Milkov, A. V., Waseda, A., Mizobe, K., & Sun, C. H. (2009). Evidence of subsurface anaerobic biodegradation of hydrocarbons and potential secondary methanogenesis in terrestrial mud volcanoes. *Marine and Petroleum Geology*, *26*, 1692–1703. https://doi.org/10.1016/j.marpetgeo.2008.12.002

Fallahi, M. J., Obermann, A., Lupi, M., Karyono, K., & Mazzini, A. (2017). The plumbing system feeding the Lusi eruption revealed by ambient noise tomography. *Journal of Geophysical Research: Solid Earth*, *122*, 8200–8213. https://doi.org/doi:10.1002/2017JB014592

Giggenbach, W. F., Sano, Y., & Wakita, H. (1993). Isotopic composition of helium, and CO_2 and CH_4 contents in gases produced along the New Zealand part of a convergent plate boundary. *Geochimica et Cosmochimica Acta*, *57*(14), 3427–3455. https://doi.org/10.1016/0016-7037(93)90549-C

Global Volcanism Program (2013). In E. Venzke (Ed.), *Volcanoes of the World*, v. 4.8.1. Smithsonian Institution. https://doi.org/10.5479/si.GVP.VOTW4-2013

Gutsalo, L. K., and A. M. Plotnikov (1981), Carbon isotopic composition in the CH_4-CO_2 system as a criterion for the origin of methane and carbon dioxide in Earth natural gases (in Russian), paper presented at Doklady Akademii Nauk SSSR (Proceedings of the USSR Academy of Science).

Hall, R. (2002). Cenozoic geological and plate tectonic evolution of SE Asia and the SW Pacific: Computer-based reconstructions, model and animations. *Journal of Asian Earth Sciences*, *20*(4), 353–431. https://doi.org/10.1016/S1367-9120(01)00069-4

Hall, R. (2013). The palaeogeography of Sundaland and Wallacea since the Late Jurassic. *Journal of Limnology*, *72*, –1, 17. https://doi.org/10.4081/jlimnol.2013.s2.e1

Hall, R., Cottam, M. A., & Wilson, M. E. J. (2011). Australia–SE Asia collision: Plate tectonics and crustal flow. In M. A. C. R. Hall, & M. E. J. Wilson (Eds.), *The SE Asian gateway: history and tectonics of Australia-Asia collision*, edited by, *Special Publications*, (Vol. 355, pp. 75–109). London: Geological Society. https://doi.org/10.1144/SP355.5

Halldórsson, S. A., Hilton, D. R., Troll, V. R., & Fischer, T. P. (2013). Resolving volatile sources along the western Sunda arc, Indonesia. *Chemical Geology*, *339*, 263–282. https://doi.org/10.1016/j.chemgeo.2012.09.042

Head, I. M., Jones, D. M., & Larter, S. R. (2003). Biological activity in the deep subsurface and the origin of heavy oil. *Nature*, *426*(6964), 344–352. https://doi.org/10.1038/nature02134

Inguaggiato, S., Mazzini, A., Vita, F., & Sciarra, A. (2018). The Arjuno-Welirang volcanic complex and the connected Lusi system: Geochemical evidences. *Marine and Petroleum Geology*, *90*, 67–76. https://doi.org/10.1016/j.marpetgeo.2017.10.015

Ishibashi, J.-I., Sato, M., Sano, Y., Wakita, H., Gamo, T., & Shanks, W. C. (2002). Helium and carbon gas geochemistry of pore fluids from the sediment-rich hydrothermal system in Escanaba Trough. *Applied Geochemistry*, *17*(11), 1457–1466. https://doi.org/10.1016/S0883-2927(02)00112-9

Istadi, B., Wibowo, H. T., Sunardi, E., Hadi, S., & Sawolo, N. (2012). Mud volcano and its evolution. *Earth Sciences, Imran Ahmad Dar, IntechOpen*, *375-434*, 861–888. https://doi.org/10.5772/24944

Istadi, B. P., Pramono, G. H., Sumintadireja, P., & Alam, S. (2009). Modeling study of growth and potential geohazard for LUSI mud volcano: East Java, Indonesia. *Marine and Petroleum Geology*, *26*, 1724–1739. https://doi.org/10.1016/j.marpetgeo.2009.03.006

Jenden, P. D., Hilton, D. R., Kaplan, I. R., & Craig, H. (Eds.) (1993). *Abiogenic hydrocarbons and mantle helium in oil and gas fields*, *United States Geological Survey, Professional Paper* (Vol. 1570, pp. 31–56).

Kamenskiy, I. L., Yakutseni, V. P., Mamyrin, B. A., Anufriyev, S. G., & Tolstikhin, I. N. (1971). Helium isotopes in nature. *Geochemistry International*, *8*, 575–589.

Kusumastuti, A., Darmoyo, A.B., Suwarlan, W., Sosromihardjo, S.P.C. (1999), The Wunut field: Pleistocene volcaniclastic gas sands in East Java, *Proceedings, Indonesian Petroleum Association, Twenty Seventh Annual Convention & Exhibition, October 1999*.

Lee, H., Muirhead, J. D., Fischer, T. P., Ebinger, C. J., Kattenhorn, S. A., Sharp, Z. D., & Kianji, G. (2016). Massive and prolonged deep carbon emissions associated with continental rifting. *Nature Geoscience*, *9*, 145–149. https://doi.org/10.1038/ngeo2622

Malvoisin, B., Mazzini, A., & Miller, S. A. (2018). Deep hydrothermal activity driving the Lusi mud eruption. *Earth and Planetary Science Letters*, *497*, 42–49. https://doi.org/10.1016/j.epsl.2018.06.006

Martha, A. A., Cummins, P., Saygin, E., Sri, W., & Masturyono (2017). Imaging of upper crustal structure beneath East Java–Bali, Indonesia with ambient noise tomography. *Geoscience Letters*, *4*(1), 14. https://doi.org/10.1186/s40562-017-0080-9

Mauri, G., Husein, A., Mazzini, A., Irawan, D., Sohrabi, R., Hadi, S., et al. (2018). Insights on the structure of Lusi mud edifice from land gravity data. *Marine and Petroleum Geology*, *90*, 104–115. https://doi.org/10.1016/j.marpetgeo.2017.05.041

Mazzini, A., & Etiope, G. (2017). Mud volcanism: An updated review. *Earth-Science Reviews*, *168*, 81–112. https://doi.org/10.1016/j.earscirev.2017.03.001

Mazzini, A., Etiope, G., & Svensen, H. (2012). A new hydrothermal scenario for the 2006 Lusi eruption, Indonesia, Insights from gas geochemistry. *Earth and Planetary Science Letters*, *317-318*, 305–318. https://doi.org/10.1016/j.epsl.2011.11.016

Mazzini, A., Nermoen, A., Krotkiewski, M., Podladchikov, Y., Planke, S., & Svensen, H. (2009). Strike-slip faulting as a trigger mechanism for overpressure release through piercement structures. Implications for the Lusi mud volcano, Indonesia. *Marine and Petroleum Geology*, *26*(9), 1751–1765. https://doi.org/10.1016/j.marpetgeo.2009.03.001

Mazzini, A., Scholz, F., Svensen, H. H., Hensen, C., & Hadi, S. (2018). The geochemistry and origin of the hydrothermal water erupted at Lusi, Indonesia. *Marine and Petroleum Geology*, *90*, 52–66. https://doi.org/10.1016/j.marpetgeo.2017.06.018

Mazzini, A., Svensen, H., Akhmanov, G. G., Aloisi, G., Planke, S., Malthe-Sørenssen, A., & Istadi, B. (2007). Triggering and dynamic evolution of the LUSI mud volcano, Indonesia. *Earth and Planetary Science Letters*, *261*(3-4), 375–388. https://doi.org/10.1016/j.epsl.2007.07.001

Milkov, A. V. (2010). Methanogenic biodegradation of petroleum in the West Siberian Basin (Russia): Significance for formation of giant Cenomanian gas pools. *AAPG Bulletin*, *94*(10), 1485–1541. https://doi.org/10.1306/01051009122

Milkov, A. V. (2011). Worldwide distribution and significance of secondary microbial methane formed during petroleum biodegradation in conventional reservoirs. *Organic Geochemistry*, *42*(2), 184–207. https://doi.org/10.1016/j.orggeochem.2010.12.003

Milkov, A. V. (2018). Secondary microbial gas. In H. Wilkes (Ed.), *Hydrocarbons, oils and lipids: Diversity, origin, chemistry and fate*, edited by, (pp. 1–10). Cham: Springer International Publishing. https://doi.org/10.1007/978-3-319-54529-5_22-1

Milkov, A. V., & Etiope, G. (2018). Revised genetic diagrams for natural gases based on a global dataset of >20,000 samples. *Organic Geochemistry*, *125*, 109–120. https://doi.org/10.1016/j.orggeochem.2018.09.002

Miller, S. A., & Mazzini, A. (2018). More than ten years of Lusi: A review of facts, coincidences, and past and future studies. *Marine and Petroleum Geology*, *90*, 10–25. https://doi.org/10.1016/j.marpetgeo.2017.06.019

Moreira, M. A., & Kurz, M. D. (2013). Noble gases as tracers of mantle processes and magmatic degassing. In P. Burnard (Ed.), *The Noble Gases as Geochemical Tracers* (pp. 371–391). Berlin, Heidelberg: Springer-Verlag.

Moscariello, A., Do Couto, D., Mondino, F., Booth, J., Lupi, M., & Mazzini, A. (2018). Genesis and evolution of the Watukosek fault system in the Lusi area (East Java). *Marine and Petroleum Geology*, *90*, 125–137. https://doi.org/10.1016/j.marpetgeo.2017.09.032

Obermann, A., Karyono, K., Diehl, T., Lupi, M., & Mazzini, A. (2018). Seismicity at Lusi and the adjacent volcanic complex, Java, Indonesia. *Marine and Petroleum Geology*, *90*, 149–156. https://doi.org/10.1016/j.marpetgeo.2017.07.033

O'Nions, R. K., & Oxburgh, E. R. (1988). Helium, volatile fluxes and the development of continental crust. *Earth and Planetary Science Letters*, *90*(3), 331–347. https://doi.org/10.1016/0012-821X(88)90134-3

Ozima, M., & Podosek, F. A. (2002). *Noble gas ceochemistry*. Cambridge: Cambridge University Press.

Panzera, F., D'Amico, S., Lupi, M., Mauri, G., Karyono, K., & Mazzini, A. (2018). Lusi hydrothermal structure inferred through ambient vibration measurements. *Marine and Petroleum Geology*, *90*, 116–124. https://doi.org/10.1016/j.marpetgeo.2017.06.017

Peters, K. E., Walters, C. C., & Moldowan, J. M. (2005). *The biomarker guide*. Cambridge: Cambridge University Press.

Poreda, R. J., Jeffrey, A. W. A., Kaplan, I. R., & Craig, H. (1988). Magmatic helium in subduction-zone natural gases. *Chemical Geology*, *71*(1-3), 199–210. https://doi.org/10.1016/0009-2541(88)90115-5

Poreda, R. J., Jenden, P. D., Kaplan, I. R., & Craig, H. (1986). Mantle helium in Sacramento basin natural gas wells. *Geochimica et Cosmochimica Acta*, *50*(12), 2847–2853. https://doi.org/10.1016/0016-7037(86)90231-0

Prinzhofer, A. (2013). Noble gases in oil and gas accumulations. In P. Burnard (Ed.), *The noble gases as geochemical tracers* (pp. 225–248). Berlin, Heidelberg: Springer.

Procesi, M., Ciotoli, G., Mazzini, A., & Etiope, G. (2019). Sediment-hosted geothermal systems: Review and first global mapping. *Earth-Science Reviews*, *192*, 529–544. https://doi.org/10.1016/j.earscirev.2019.03.020

Sakata, S., Sano, Y., Maekawa, T., & Igari, S.-I. (1997). Hydrogen and carbon isotopic composition of methane as evidence for biogenic origin of natural gases from the Green Tuff Basin, Japan. *Organic Geochemistry*, *26*(5-6), 399–407. https://doi.org/10.1016/S0146-6380(97)00005-3

Samankassou, E., Mazzini, A., Chiaradia, M., Spezzaferri, S., Moscariello, A., & Do Couto, D. (2018). Origin and age of carbonate clasts from the Lusi eruption, Java, Indonesia. *Marine and Petroleum Geology*, *90*, 138–148. https://doi.org/10.1016/j.marpetgeo.2017.11.012

Sano, Y., & Fischer, T. P. (2013). The analysis and interpretation of noble gases in modern hydrothermal systems. In P. Burnard (Ed.), *The noble gases as geochemical tracers*, edited by, (pp. 249–317). Berlin, Heidelberg: Springer Berlin Heidelberg. https://doi.org/10.1007/978-3-642-28836-4_10

Sano, Y., Gamo, T., & Williams, S. N. (1997). Secular variations of helium and carbon isotopes at Galeras volcano, Colombia. *Journal of Volcanology and Geothermal Research*, *77*(1-4), 255–265. https://doi.org/10.1016/S0377-0273(96)00098-4

Sano, Y., & Wakita, H. (1985). Geographical distribution of $^{3}He/^{4}He$ ratios in Japan: Implications for arc tectonics and incipient magmatism. *Journal of Geophysical Research*, *90*(B10), 8729–8741. https://doi.org/10.1029/JB090iB10p08729

Satyana, A. H., & Purwaningsih, M. E. M (2003a), Geochemistry of the East Java Basin: New observations on oil grouping, genetic gas types and trends of hydrocarbon habitats, *Proceedings of the 29th IAGI Annual Convention and Exhibition*.

Satyana, A. H., Purwaningsih, M. E. M. (2003b), Oligo-Miocene carbonates of Java: Tectonic setting and effects of volcanism, *Proceedings of the 32nd IAGI and 28th HAGI Annual Convention and Exhibition*.

Schoell, M. (1983), Genetic characterization of natural gases. American Association of Petroleum Geologists Bulletin paper presented at American Association of Petroleum Geologists Bulletin.

Sciarra, A., Mazzini, A., Inguaggiato, S., Vita, F., Lupi, M., & Hadi, S. (2018). Radon and carbon gas anomalies along the Watukosek Fault System and Lusi mud eruption, Indonesia. *Marine and Petroleum Geology*, *90*, 77–90. https://doi.org/10.1016/j.marpetgeo.2017.09.031

Sharaf, E., Simo, J. A., Carroll, A. R., & Shields, M. (2005). Stratigraphic evolution of Oligocene–Miocene carbonates and siliciclastics, East Java basin, Indonesia. *AAPG Bulletin*, *89*(6), 799–819. https://doi.org/10.1306/01040504054

Smyth, H. R., Hall, R., & Nichols, G. J. (2008). Cenozoic volcanic arc history of East Java, Indonesia: The stratigraphic record of eruptions on an active continental margin. In A. E. Draut, P. D. Clift, & D. W. Scholl (Eds.), *Formation and Applications of the Sedimentary Record in Arc Collision Zones* (pp. 199–222).Boulder, CO: Geological Society of America.

Snyder, G., Poreda, R., Fehn, U., & Hunt, A. (2003). Sources of nitrogen and methane in Central American geothermal settings: Noble gas and 129I evidence for crustal and magmatic volatile components. *Geochemistry, Geophysics, Geosystems*, *4*(1), 9001. https://doi.org/10.1029/2002GC000363

Sutrisna, E. (2009), "Can LUSI be stopped?—A case study and lessons learned from the relief wells", *Eos Transactions American Geophysical Union*, *90*(52), Fall Meet. Suppl., Abstract NH51A-1053. https://doi.org/10.1029/eost2009eo52

Svensen, H. H., Iyer, K., Schmid, D. W., & Mazzini, A. (2018). Modelling of gas generation following emplacement of an igneous sill below Lusi, East Java, Indonesia. *Marine and Petroleum Geology*, *90*, 201–208. https://doi.org/10.1016/j.marpetgeo.2017.07.007

Tingay, M. (2015). Initial pore pressures under the Lusi mud volcano, Indonesia. *Interpretation*, *3*(1), SE33–SE49. https://doi.org/10.1190/int-2014-0092.1

Van Noorden, R. (2006). Mud volcano floods Java. In *Nature News*. Italy:University of Padua. https://doi.org/10.1038/news060828-1

Vanderkluysen, L., Burton, M. R., Clarke, A. B., Hartnett, H. E., & Smekens, J.-F. (2014). Composition and flux of explosive gas release at LUSI mud volcano (East Java, Indonesia). *Geochemistry, Geophysics, Geosystems*, *15*, 2932–2946. https://doi.org/10.1002/2014gc005275

Wenger, L. M., Davis, C. L., & Isaksen, G. H. (2002). Multiple controls on petroleum biodegradation and impact on oil quality. *SPE Reservoir Evaluation and Engineering*, *5*(05), 375–383. https://doi.org/10.2118/80168-PA

Whiticar, M. J., Faber, E., & Schoell, M. (1986). Biogenic methane formation in marine and freshwater environments: CO_2 reduction vs. acetate fermentation—Isotope evidence. *Geochimica et Cosmochimica Acta*, *50*(5), 693–709. https://doi.org/10.1016/0016-7037(86)90346-7

Xu, S., Nakai, S. I., Wakita, H., Xu, Y., & Wang, X. (1995). Helium isotope compositions in sedimentary basins in China. *Applied Geochemistry*, *10*(6), 643–656. https://doi.org/10.1016/0883-2927(95)00033-X